



Optically imageable metastatic model of human breast cancer

Xiaoming Li¹, Jinwei Wang¹, Zili An¹, Meng Yang¹, Eugene Baranov¹, Ping Jiang¹, Fangxian Sun¹, A.R. Moossa² & Robert M. Hoffman^{1,2}

¹AntiCancer, Inc., San Diego, California, USA; ²Department of Surgery, University of California, San Diego, California, USA

Received 26 November 2001; accepted in revised form 27 December 2001

Key words:

Abstract

We report an optically imageable orthotopic metastatic nude mouse model of the human breast cancer MDA-MB-435 expressing green fluorescent protein (GFP). We demonstrate fluorescent imaging of primary and metastatic growth in live tissue and in intact animals. Fragments of tumor tissue expressing GFP were sutured into the pocket in the right second mammary gland. Tumor tissue was strongly fluorescent, enabling whole-body imaging of tumor growth by week 5. Neovascularization of the primary tumor was also visualized by whole-body imaging by contrast of the vessels to the fluorescent tumor. At autopsy, the MDA-MB-435-GFP was found to have metastasized to various organs, including the lung in 55% of the animals, the lymph nodes in 15% of the animals including axillary nodes, and the liver in 10% of the animals. These metastases could be visualized in fresh tissue by fluorescent imaging. Detailed fluorescence analysis visualized extensive metastasis in the thoracic cavity and the lymphatic system. Large metastatic nodules in the lung involved most of the pulmonary parenchyma in all lobes. Lymph node metastasis was found mainly in the axillary area. In the liver, fluorescent macroscopic metastatic nodules were found under the capsule. The metastatic pattern in the model thus reflected clinical metastatic breast cancer and provides a powerful model for drug discovery for this disease.

Abbreviations: GFP – green fluorescent protein; SOI – surgical orthotopic implantation

Introduction

We have previously reported on the use of the *Aequorea victoria* green fluorescent protein (GFP) for studying tumor growth and metastasis *in vivo* [1, 2]. In this study, we report a novel optically imageable orthotopic metastatic nude mouse model of the human breast cancer MDA-MB-435 expressing GFP. We demonstrate fluorescent imaging of primary and metastatic growth in live tissue and in intact animals.

Materials and methods

Female athymic *nu/nu* mice, 4–5 weeks old, were used in the study. Mice were fed with autoclaved laboratory rodent diet (Tecklad LM-485, Western Research Products, Orange, California). All animal studies were conducted in accordance with the principles and procedures outlined in the National Institutes of Health Guide for the Care and Use of Laboratory Animals under assurance number A3873-1.

MDA-MB-435, an ER-negative cell line isolated from the pleural effusion of a 31-year-old female with metasta-

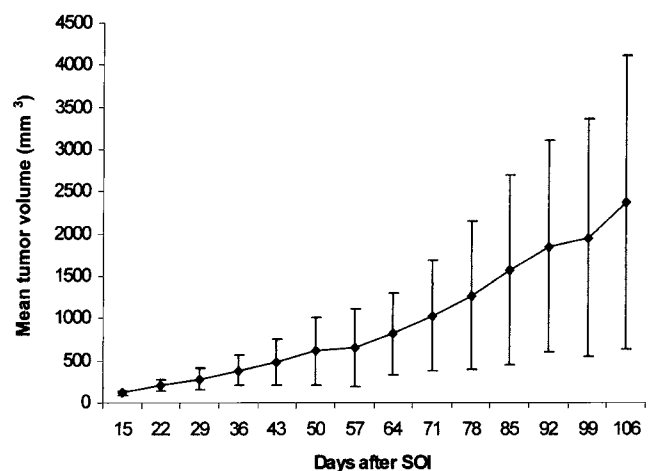


Figure 1. Primary tumor growth curve. Human breast carcinoma cell line MDA-MB-435 with GFP expression was implanted orthotopically in nude mice using the surgical orthotopic implantation (SOI) technique. See 'Materials and methods' for details. Tumor was measured by the smallest (a) and the largest (b) dimensions with a pair of calipers. Tumor volume was calculated by the formula: $a^2 \times b/2$.

tic ductal adenocarcinoma of the breast [3,4], was purchased from ATCC (Rockville, Maryland). Cryopreserved cells were thawed and maintained in monolayer culture in

Correspondence to: Dr R.M. Hoffman, AntiCancer, Inc., 7917 Ostrow Street, San Diego, CA 92111, USA. Tel: +1-858-654-2555; Fax: +1-858-268-4175; E-mail: all@anticancer.com

Figure 2. Whole-body fluorescent images of a typical orthotopic primary tumor at different growth stages. Solid arrows indicate primary tumor. (a) 14-day tumor. (b) 42-day tumor (hollow arrow indicates invasion). (c) 70-day tumor (orange arrow indicates neovascularization). (d) 98-day tumor (orange arrow indicates neovascularization). Bar = 1 cm.

Figure 3. Fluorescent images of metastasis in live tissue. (a) Numerous metastases (solid arrows) in the lungs (hollow arrows) of nude mice. Bar = 1 mm. (b) Large metastatic nodules in the lungs involving most of the pulmonary parenchyma (solid arrows), and metastases to the parietal pleura (hollow arrows). Bar = 1 mm. (c) Large metastatic nodule in the axillary lymph node (solid arrow). Bar = 0.5 cm. (d) Metastasis (solid arrow) under the capsule of the liver (hollow arrows). Bar = 1 mm.

Figure 4. Microscopic view of metastasis of GFP-MDA-MB-435. (a) Lung metastasis of GFP-MDA-MB-435 (arrow). (b) Lymph node metastasis (arrow). (c) Liver metastasis (arrows). Bar = 25 μm .

Dulbecco's modified essential medium supplemented with 10% fetal bovine serum, sodium pyruvate, L-glutamine, non-essential amino acids and a two-fold concentration of vitamins (GIBCO, Grand Island, New York). The cultures were incubated at 37 °C in a humidified atmosphere of 5% CO₂ and 95% air. Cells were examined with commercially available kits and found free of viruses (Microbiological Associates, Walkersville, Maryland) and *Mycoplasma* (Gen-Probe, Inc., San Diego, California).

The RetroXpress vector pLEIN, containing vector expressing enhanced green fluorescent protein (EGFP), was purchased from CLONTECH Laboratories, Inc. (Palo Alto, California). PT67, an NIH3T3-derived packaging cell line (Palo Alto, California), was used to package the retrovirus. 20%-confluent MDA-MB-435 cells were incubated with a 1:1 precipitated mixture of retroviral supernatants of PT67 cells for 72 h. The selective medium containing G418 was stepwise increased (400, 600, 800 and 1,000 $\mu\text{g}/\text{ml}$) in the MDA-MB-435 cell cultures. The brightest MDA-MB-435 clones expressing GFP were selected, combined, and then amplified by conventional culture methods.

Tumor cells with GFP expression were harvested by washing the monolayer with HBSS, followed by a brief incubation in 0.25% trypsin and 0.02% EDTA. The cells were then collected, washed twice by centrifugation and resuspended in HBSS. Cell number and viability were determined by staining a small volume of cell suspension with a 0.2% trypan blue saline solution and examining the cells in a hemocytometer. Subcutaneous injection of the cells into the flanks of female nude mice was carried out with 2×10^6 cells per mouse.

Subcutaneously growing tumors with high GFP expression were harvested in log phase. The periphery of the tumors, free of necrosis, was trimmed off and used for SOI. The tissues were cut into 1-mm³ pieces. The resulting tumor tissue fragments were mixed thoroughly before implantation to insure that all the mice were implanted with equally viable tissue.

Surgical orthotopic implantation was then performed as follows: Twenty mice were anesthetized with isoflurane inhalation and put in a supine position. The right second mammary gland was chosen for orthotopic implantation. A small incision was made along the medial side of the nipple. The mammary fat pad was exposed through blunt dissection. A small cut was made on the fat pad and then bluntly expanded to form a small pocket. Four pieces of tumor tissue, previously prepared as described above, were sutured into the pocket using an 8-0 nylon suture. The skin was closed

Table 1 Metastatic incidence of GFP-MDA-MB-435 after SOI in nude mice.

	Distant metastasis		
	Lung	Lymph node	Liver
Incidence	3/20 (15%)	11/20 (55%)	2/20 (10%)

GFP-gene transfected human breast cancer MDA-MB-435 was implanted orthotopically in nude mice using the surgical orthotopic implantation (SOI) technique (See 'Materials and methods' for details). All animals were sacrificed at day 106 after implantation. Samples from the lung, the lymph node and the liver were processed for standard H&E staining and subsequently examined microscopically.

with a 6-0 silk suture. All procedures [5] were carried out under a 5 \times dissecting microscope.

A Leica fluorescence stereo microscope model LZ12 equipped with a mercury 50W lamp power supply was used for imaging animals with GFP-expressing tumors [6]. Selective excitation of GFP was produced through a D425/60 band-pass filter and 470 DCXR dichroic mirror. Emitted fluorescence was collected through a long-pass filter GG475 (Chroma Technology, Brattleboro, Vermont) on a Hamamatsu C5810 3-chip cooled color CCD camera (Hamamatsu Photonics Systems, Bridgewater, New Jersey). Images were processed for contrast and brightness and analyzed with the use of Image Pro Plus 3.1 software (Media Cybernetics, Silver Springs, Maryland). High resolution images of 1024 \times 724 pixels were captured directly on an IBM PC or continuously through video output on a high resolution Sony VCR model SLV-R1000 (Sony Corp., Tokyo, Japan).

Results and discussion

The orthotopic primary tumors were approximately 112 mm³ at 14 days post-SOI and by day-106, tumor size reached 2.4 cm³ (Figure 1). Tumor tissue was strongly fluorescent due to GFP expression, enabling whole-body imaging [6] of tumor growth (Figure 2). Local invasion was visualized at week 5 by whole-body imaging (Figure 2B). Neovascularization of the primary tumor was demonstrated [7] by whole-body imaging by contrast to the fluorescent tumor (Figures 2C and D).

The MDA-MB-435-GFP metastasized to various organs, including the lung in 55% of the animals, the lymph nodes in 15% of the animals including axillary nodes, and the liver in 10% of the animals (Table 1). These metastases could be visualized in fresh tissue by fluorescence imaging.

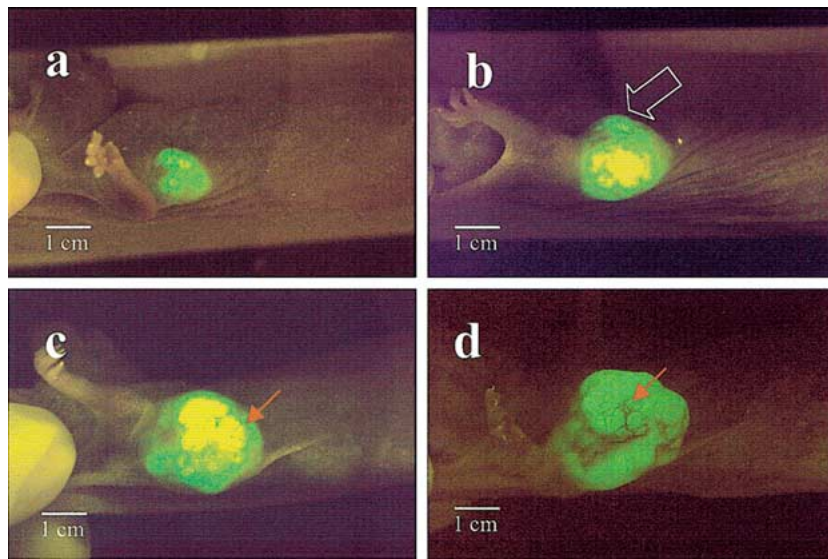


Figure 2.

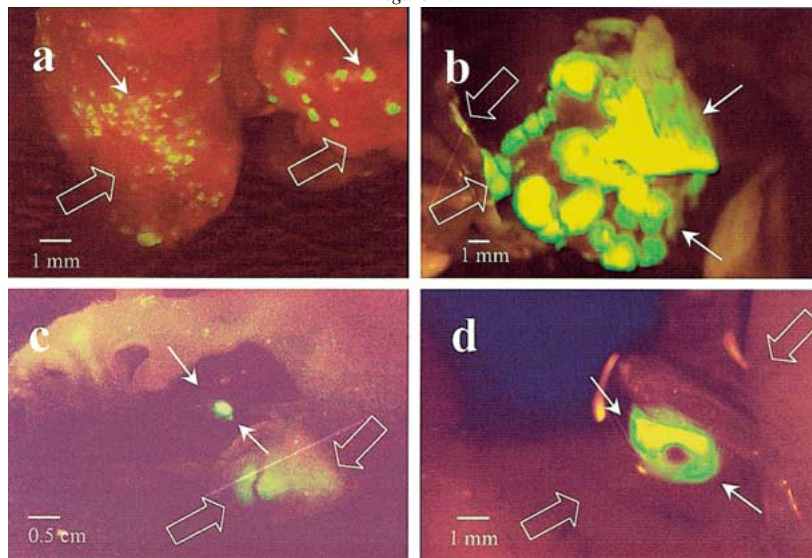


Figure 3.

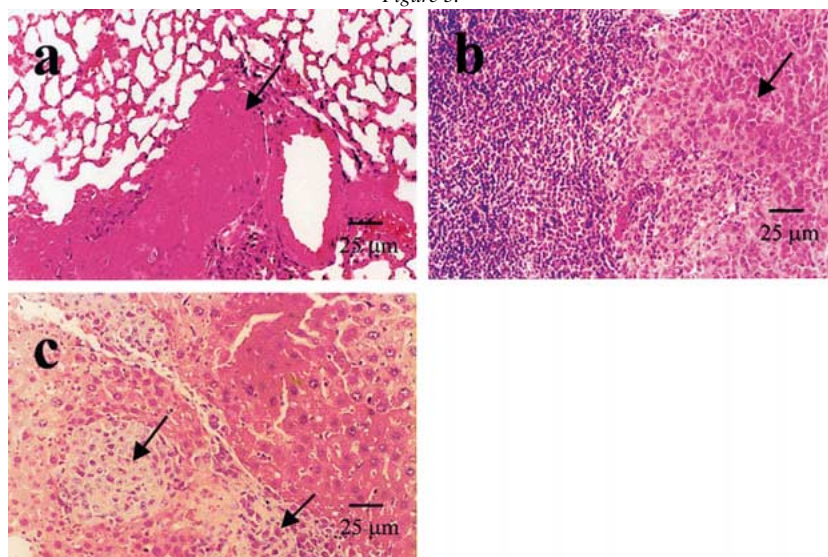


Figure 4.

Detailed fluorescence analysis visualized extensive metastasis in the thoracic cavity and the lymphatic system. Large metastatic nodules in the lung involved most of the pulmonary parenchyma in all lobes (Figures 3A and B). In the mice examined, almost no normal lung tissue could be seen due to extensive metastases (Figure 3B). Microscopically, large metastatic nests were profusely distributed in the lung squeezing the alveoli and bronchioles (Figure 4A). Metastatic nodules were also found on the surface of the parietal pleura (Figure 3B). The diaphragm was extensively invaded in some mice. Lymph node metastasis was found mainly in the axillary area (Figures 3C, 4B). In the liver, fluorescent macroscopic metastatic nodules were found under the capsule (Figure 3D). Microscopically, metastatic nests were profusely distributed in the liver parenchyma (Figure 4C). The metastatic pattern in the model thus reflected clinical metastatic breast cancer.

Previous studies for orthotopic implantation of MDA-MB-435 used cell suspension injection [8–13] instead of orthotopic tissue fragment implantation as reported in the present study. Previous studies did not observe liver metastasis for this cell line in nude mice. Our model reported here revealed that the human breast cancer cell line MDA-MB-435-GFP was capable of metastasizing to the liver in nude mice.

The integration of GFP-expression in this model allowed us to monitor the primary and metastatic tumor growth with fluorescence imaging including real-time whole-body imaging of intact animals. This new feature enables real-time imaging of breast tumor growth, metastasis, and angiogenesis suitable for numerous applications including screening and evaluation of agents active against these processes.

Acknowledgement

This study was supported in part by the National Cancer Institute grant 1 R43 CA89779-01.

References

1. Chishima T, Miyagi Y, Wang X et al. Cancer invasion and micrometastasis visualized in live tissue by green fluorescent protein expression. *Cancer Res* 1997; 57: 2042–7.
2. Hoffman RM. Green fluorescent protein to visualize cancer progression and metastasis. In Conn PM (ed): *Methods in Enzymology. Green Fluorescent Protein*. San Diego: Academic Press 1999; Vol. 302: 20–31.
3. Bagheri-Yarmand R, Kourbali Y, Rath AM et al. Carboxymethyl benzylamide dextran blocks angiogenesis of MDA-MB435 breast carcinoma xenografted in fat pad and its lung metastases in nude mice. *Cancer Res* 1999; 59: 507–10.
4. Price JE, Polyzos A, Zhang RD et al. Tumorigenicity and metastasis of human breast carcinoma cell lines in nude mice. *Cancer Res* 1990; 50: 717–21.
5. Fu X, Le P, Hoffman RM. A metastatic orthotopic-transplant nude-mouse model of human patient breast cancer. *Anticancer Res* 1993; 13: 901–4.
6. Yang M, Baranov E, Jiang P et al. Whole-body optical imaging of green fluorescent protein-expressing tumors and metastases. *Proc Natl Acad Sci USA* 2000; 97: 1206–11.
7. Yang M, Baranov E, Li X-M et al. Whole-body and intravital optical imaging of angiogenesis in orthotopically implanted tumors. *Proc Natl Acad Sci USA* 2001; 98: 2616–21.
8. Bao L, Matsumura Y, Baban D et al. Effects of inoculation site and Matrigel on growth and metastasis of human breast cancer cells. *Br J Cancer* 1994; 70: 228–32.
9. Glinsky GV, Price JE, Glinsky VV et al. Inhibition of human breast cancer metastasis in nude mice by synthetic glycoamines. *Cancer Res* 1996; 56: 5319–24.
10. Price JE. Metastasis from human breast cancer cell lines. *Breast Cancer Res Treat* 1996; 39: 93–102.
11. Rose DP, Connolly JM, Coleman M. Effect of omega-3 fatty acids on the progression of metastases after the surgical excision of human breast cancer cell solid tumors growing in nude mice. *Clin Cancer Res* 1996; 2: 1751–6.
12. Schmidt CM, Settle SL, Keene JL et al. Characterization of spontaneous metastasis in an aggressive breast carcinoma model using flow cytometry. *Clin Exp Metastasis* 1999; 17: 537–44.
13. Wang CY, Chang YW. A model for osseous metastasis of human breast cancer established by intrafemur injection of the MDA-MB-435 cells in nude mice. *Anticancer Res* 1997; 17: 2471–4.